Biomedicine & Pharmacotherapy 121 (2020) 109678

Contents lists available at ScienceDirect

Biomedicine & Pharmacotherapy

journal homepage: www.elsevier.com/locate/biopha

Nucleosome binding peptide presents laudable biophysical and *in vivo* effects

Kaian Teles[a], Vinicius Fernandes[a,b], Isabel Silva[a], Manuela Leite[a], Cesar Grisolia[c], Vincenzo R. Lobbia[d], Hugo van Ingen[d], Rodrigo Honorato[e], Paulo Lopes-de-Oliveira[e], Werner Treptow[b], Guilherme Santos[a,*]

[a] Laboratório de Farmacologia Molecular, Departamento de Farmácia, Universidade de Brasília, Brasília, 70919-970, Brazil
[b] Laboratório de Biologia Teórica e Computacional, Departamento de Biologia Celular, Universidade de Brasília, DF, 70910-900, Brasília, Brazil
[c] Laboratório de Genética Toxicológica, Departamento de Genética e Morfologia, Instituto de Ciências Biológicas, Universidade de Brasília, Brasília, Brazil
[d] NMR Spectroscopy Group, Bijvoet Center for Biomolecular Research, Utrecht University, Padualaan 8, 3584 CH, Utrecht, the Netherlands
[e] Laboratório Nacional de Biociências (LNBio), Campinas, SP, Brazil

ARTICLE INFO

Keywords:
Peptides
Nucleosome
Chromatin

ABSTRACT

Chromatin state is highly dependent on the nucleosome binding proteins. Herein, we used a multipronged approach employing biophysical and *in vivo* experiments to characterize the effects of Nucleosome Binding Peptides (NBPeps) on nucleosome and cell activity. We performed a series of structure-based calculations on the nucleosome surface interaction with GMIP1 (a novel NBPep generated in silico), and HMGN2 (nucleosome binding motif of HMGN2), which contains sites that bind DNA and the acid patch, and also LANA and H4pep (nucleosome binding motif of H4 histone tail) that only bind to the acidic patch. Biochemical assays shows that H4pep, but not HMGN2, GMIP1 and LANA, is highly specific for targeting the nucleosome, with important effects on the final nucleosome structure and robust *in vivo* effects. These findings suggest that NBPeps might have important therapeutic implications and relevance as tools for chromatin investigation.

1. Introduction

Chromatin is a macromolecular complex composed of distinct molecules. Highly basic proteins (histone octamer) interact with DNA to form the nucleosome core particle (NCP), generating the fundamental repetitive unit of chromatin. The NCP represents the first level of DNA compaction, followed by a cooperative nucleosome interaction to form the higher-order chromatin structure (reviewed in [1]). Chromatin dynamics, which is controlled by a plethora of Nucleosome Binding Proteins (NBPs), is essential for genome integrity and gene expression regulation. From condensed to relaxed chromatin, NBPs may induce specific modifications of chromatin architecture dependent on their unique properties [2]. In addition to NBPs, the nuclear environment also comprises many small molecules with different chemical natures that can directly interact with nucleosomes, such as Mg^{2+} and lipids [3,4].

The nucleosome core particle surface contains the acidic patch, a highly negative region formed by six residues of H2A and two of H2B, that is responsible for nucleosome–nucleosome interactions and is a target for several NBPs [2]. The first structure of a nucleosome:peptide complex showed at atomic level the binding mode of the viral peptide LANA to the acidic patch [5]. In the following years, other nucleosome:NBPs complex structures were solved, revealing the atomic details of the interaction of NBPs with the nucleosome surface, highlighting the acidic patch as the principal protein-docking region [6].

Unlike canonical drug targets such as enzymes or protein receptors, the nucleosome is a structural protein:DNA complex without typical druggable cavities, and this impedes research for new exogenous nucleosome binding molecules. Instead of focusing on small molecules for occupying the nucleosome surface, we try to understand and developed more complex molecules, such as the Nucleosome Binding Peptides (NBPeps).

Herein, we characterized the effects of NBPeps on nucleosome and chromatin structure. Firstly, we designed and generated *in silico* a novel NBPep, GMIP1, with nucleosome surface binding highly dependent on the DNA. Then, in order to understand how NBPeps with distinct nucleosome binding sites affect nucleosome structure, we performed a series of structure-based calculations on the nucleosome surface interaction to the NBPeps. We studied four NBPeps, GMIP1 and HMGN2 (the nucleosome binding motif from HMGN2), which contains sites that

* Corresponding author.
E-mail address: gsantos@unb.br (G. Santos).

https://doi.org/10.1016/j.biopha.2019.109678
Received 27 September 2019; Received in revised form 30 October 2019; Accepted 13 November 2019

bind DNA and the acid patch, and also LANA and H4pep (structure-based nucleosome binding motif derived from the N-terminal domain of histone H4) that only bind to the acidic patch. Interestingly, we observed that NBPeps induced specific atomic fluctuations of the nucleosome structure. *In vitro* studies corroborate the idea that NBPeps may affect the stability of the nucleosome structure, however only H4pep showed high nucleosome binding affinity and specific actions on the final nucleosome structure while HMGN2, LANA and GMIP1 peps seems to be non-specific DNA interactors, based on oppositely charged residues. Cell-based assays showed that the four NBPeps penetrated the cell, localizing at the nuclear environment and, except GMIP1, interfered with tumor cell viability. However, beside the non specific properties on the nucleosome, apart from H4pep, the fish embryo toxicity (FET) test showed that the four NBPeps could cause tissue modifications, such as defects in pigmentation and induction of earlier hatching.

2. Methods

2.1. In silico NBPep design

KV finder software with a PyMOL interface plugin (The PyMOL – Molecular Graphics System Version 1.3 Schrodinger, LLC) was used to define the cavities on the nucleosome:protein complex. YSARA software was used for the GMIP1 design and the optimized conformation by minimizing energy was performed using the force field YAMBER3.

2.2. NBPeps

All Peptides were bought from Biomatik with purity > 95 % and diluted in MiliQ H_2O. Fluorescent peptides were bought with TAMRA -(559/583 nm) in the N-terminus. The concentration was determined by spectrophotometric method as described in [7]. All peptides are described in the supplementary table 1.

2.3. Recombinant H2A-H2B for NMR

BL21(DE3)pLysS cells were used to express *Xenopus laevis* H2A or H2B in deuterated M9 medium containing 2 g/l (12C-2D) D-glucose (1,2,3,4,5,6,6-d7) and 0.5 g/L 15NHCl. One hour before induction with 1 mM IPTG, 60 mg/L α-ketobutyric acid (4–13 C,3,3-2d) and 80 mg/L α-ketoisovalerate (3-(methyl-d3),4–13 C,3-d) sodium salt were added to the medium. Histones were purified as described by Dyer et al. [8] To refold dimers, H2A and H2B were mixed in equimolar ratio in unfolding buffer (7 M urea, 150 mM NaCl, 50 mM NaPi, 1 mM EDTA, pH 7.5) and dialysed against high salt buffer (2 M NaCl, 10 mM Tris, 1 mM EDTA, pH 7.5). Dimers were purified using size exclusion chromatography (Hiload superdex 200 16/600) and then dialysed against low salt buffer (20 mM NaPi, 0.01 % NaN_3, pH6.2).

2.4. In vitro chromatin fibers and nucleosome reconstitution

Histone octamers (HO) were purified from chicken erythrocyte nuclei as described in Huynh, V. A. T., P. J. J. Robinson, and D. Rhodes, 2005. 601 DNA Widom with 167 base pairs (bp) was used to reconstitute mononucleosomes and array 177.36 was used to reconstitute 10 nm chromatin fibers, both using the slow salt dialysis method as described in Huynh et al. (2005) [9]. The analyses of the reconstitution were verified by electrophoresis in native bis-acrylamide gels (6 %) or agarose gels (0.8 %).

2.5. Mononucleosome precipitation

Freshly reconstituted mononucleosomes (115 nM mononucleosome, Tris 10 mM pH 7.4, EDTA 1.5 mM NaCl 15 mM) were incubated with specified concentration of NBPeps for 30 min at room temperature. The samples were centrifuged (Sigma centrifuge-2K15) at 15,493 x g for 20 min at 25 °C. The supernatant was transferred to another micro-centrifuge tube and the pellet was resuspended in the same buffer as the mononucleosome. The samples were analyzed by electrophoresis in native 6 % bis-acrylamide gel carried out with 0.5 × TBE buffer at 15 mA. Densitometry was performed using ImageJ (National Institute of Health, Bethesda, MD, USA) version 1.49.

2.6. DNA binding assay

Widom 601 DNA fragments containing 167bp (30 nM DNA, 10 mM Tris pH 7.4, 135 mM NaCl) were incubated with specified concentrations of GMIP1 for 2 h at 37 °C and 100 RPM. The analysis was done in 0.8 % agarose gel in TBE 0.5 × . Samples were loaded with 30 % glycerol, to avoid interaction caused by phenol blue and GMIP1.

2.7. Nucleosome binding assay

Freshly reconstituted mononucleosomes (115 nM mononucleosome, Tris 10 mM pH 7.4, EDTA 1.5 mM NaCl 15 mM) were incubated with specified concentration of fluorescent NBPeps for 120 min at room temperature. Then samples were analyzed by electrophoresis in native 6 % bis-acrylamide gel carried out with 0.5 × TBE buffer at 15 mA. Gels were analyzed using Amersham Imager 600 (GE) with the RGB laser kit detection for 520 nm, to visualize the peptide, following incubation in ethidium bromide bath and analyzed with UV for ethidium bromide detection. For Kd determination, band densitometry was performed in the gel reveled with 520 nm laser, using ImageJ (National Institute of Health, Bethesda, MD, USA) version 1.49, followed by analysis in Prism 6 Graphpad software using Binding - saturation binding to total and non-specific template.

2.8. Chromatin compaction assay

Chromatin compaction by Mg^{2+} was adapted from Rhodes Lab protocol [10]. Briefly, assembled chromatin fibers were incubated with vehicle (10 mM Tris−HCl (pH 7.5) or peptides (150μM GMIP1 or H4pep) for 2 h in room temperature. Next, 3 mM $MgCl_2$ were added, incubated for 15 min on ice and centrifuged at 13,000 rpm for 15 min at 4 °C. The supernatants and pellets were verified by electrophoresis in native 0.8 % agarose gels, carried out with 0.2x TBE (18 mM Tris-borate, pH 8; 0.4 mM EDTA) electrophoresis buffer at 20 mA. Densitometry was performed using ImageJ (National Institute of Health, Bethesda, MD, USA) version 1.49.

2.9. Thermal shift assay

Thermalshift assay with NBPeps was adapted from Taguchi et al. [11]. Briefly, freshly reconstituted mononucleosomes (86 nM), in 10 mM Tris pH 7.4, 1.5 mM EDTA and 15 mM NaCl, were incubated with specified concentration of NBPeps for 30 min at room temperature. Next 1 mM dithiothreitol and 5X of SYPRO-Orange (SIGMA–ALDRICH) were added and incubated for 1 min at room temperature. Fluorescence was measured with a StepOnePlus Real-Time PCR unit (Applied Biosystems) with increases of 1 °C step from 25 °C to 95 °C. The fluorescence was detected at 570 nm. The Raw data was normalized using Graphpad Prism 6 software and for the determination of the temperature of melting (Tm) was obtained from the first derivative curve of the data.

2.10. MTT

For MTT assays, 8000 Hela cells or ccd10595k cells were plated in 96-well culture plates and maintained at 37 °C and 5 % CO_2 in DMEM medium with 10 % fetal bovine serum, penicillin (100U/mL) and streptomycin (100ug/mL) for 24 h. Next, wells were washed 3 times

with PBS 1X and filled with 100 u L of DMEM medium as described above containing the specified amount of NBPeps and incubated for 24 h in the same conditions. The 3-(4,5-dimethylthiazol-2-yl)-2,5-diphenyltetrazolium bromide (MTT) at 5 mg/mL was added to the wells (10 u L) and incubated for 4 h at 37∘C and 5 % CO_2. The wells were drained and the formazan crystals were solubilized in 100 u L of acidic isopropanol solution (52 u L of HCl 37 % to 12 mL of isopropanol) and agitated for 30 min at room temperature. Absorbance at 570 nm was determined with a plate spectrophotometer (DTX 800 Multimode Detector - Beckman Coulter) at 570 nm.

2.11. Flow cytometry

70.000 Hela cells were plated in 12-wells culture plates for 16 h and maintained at 37 °C and 5 % CO_2 in DMEM medium with 10 % fetal bovine serum, penicillin (100U/mL) and streptomycin (100ug/mL). Prior to treatment with NBPeps, cells were incubated for 1 h at 37 or 4 °C. Next, cells were washed with 1X PBS and filled with DMEM medium with the specified amount of fluorescent NBPeps and incubated at 37 or 4 °C for the 1 or 3 h. Wells were washed 3 times with ice cold 1X PBS and filled with 500 u L 1X PBS, cells were harvested with a cell scraper and analyzed by flow cytometry on FACSCalibur (BD biosciences). Hela cells were gated to isolate the main population of living cells from cell debris. Data analysis was done using flowjo 8.7 software.

3. Fluorescence confocal microscopy analysis

i) **Peptide cell penetration**: confluent Hela cells were treated with increased concentrations (0,1; 0,5; 1μM) of peptide GMIP1-TAMRA or vehicle (10 mM Tris − HCl) for 24 h. Next, plates were rinsed three times in PBS and fixed in formalin 3.7 % at room temperature for 10 min. Samples were rinsed three times in PBS and incubated with DAPI (300 ng/ml) for 5 min to stain nuclei. Finally, cells were rinsed three more times in PBS. Images were acquired using a laser scanning confocal microscope Leica TCS SP5. To visualize peptide localization, Z-planes of 0.20 mm thickness were acquired. The images were analyzed with LAS AF software (Leica Microsystems CMS GmbH).

ii) **Determination of peptide internalization**: two plates of 24 wells with confluent Hela cells were rinsed with DMEM without fetal bovine serum twice and maintained in PBS for 15 min in a 5 % CO2 humidified atmosphere at 37 °C. One plate was then maintained for 10 min at 4 °C. Next, the two plates were treated with GMIP1-TAMRA (1μM) of vehicle for 5, 15 and 30 min. After each treatment samples were fixed in formalin 3.7 % at room temperature for 1 h. Samples were rinsed three times in PBS and incubated with DAPI (300 ng/ml) for 5 min to stain nuclei. Finally, cells were rinsed three more times in PBS. Images were acquired using a laser scanning confocal microscope Leica TCS SP5. To visualize peptide localization, Z-planes of 0.20 mm thickness were acquired. The software LAS AF (Leica Microsystems CMS GmbH) was used for analyse images.

3.1. Zebrafish husbandry and embryo collection

Zebrafish *(Danio rerio)* were raised in an aquatic facility (ZebTec - Tecniplast, Italy) with a photoperiod cycle of 12:12 h (light:dark) at the University of Brasilia (Brazil). The water parameters were: temperature was maintained at 27.0 ± 1 °C, conductivity at 650 ± 100 μS/cm, pH at 7.0 ± 0.5 and dissolved oxygen ≥ 95 % saturation. Zebrafish embryos were collected immediately after natural mating, rinsed in water, and checked under a stereomicroscope (Stereoscopic Zoom Microscope – Stemi 2000, Zeiss, Germany). The unfertilized eggs and those showing cleavage irregularities or injuries were discarded [12].

3.2. Fish embryo toxicity (FET)

FET was adapted from Morash et al. [13]. Briefly, Zebrafish embryos at 4, 28 and 52 h post fertilization (hpf) were used to evaluate the toxicity of NBPeps in 96-well plates. Each peptide was tested at 0.1, 1, 10 and 100 u M in 100 u L of water from aquarium system; pH in all conditions was tested using pH strips (92,120 – MACHEREY-NAGEL). Embryos were stored at 27 °C with 14 h light 10 h dark cycle and evaluated Stemi 508 (Carl Zeiss) microscope with 1 and 24 h of treatment. Embryos were assessed for pigmentation, development, hatching and lethality. 10 embryos were used for each condition, if the control group showed any alteration, the plate was discarded, alterations > 10 % were considered significant and were documented using Axiocam Erc 5 s (Carl Zeiss) and ZEN software (Carl Zeiss).

3.3. Fluorescence fish embryo

Zebrafish larvae with 80 hpf were incubated with fluorescent NBPeps with specified concentration for 3 h in 100 u L in a 96-plate, larvae were washed 3 times in 100 mL to remove the excess of NBPep, imaging was done using Axioskop 2 (Carl Zeiss) with HBO 100 lamps, Axiocam Erc 5 s (Carl Zeiss) and ZEN software (Carl Zeiss) with appropriate laser filter for TAMRA (filter 4).

3.4. Fluorescence blood smear

Adults Zebrafish at 2 years old were inject in the abdomen with 50 u L, 1 mM of fluorescent NBPeps, and kept protected from light at 27 °C for 18 h. Blood was extracted from the fins using a pipet tip and heparin 250 IU to make the blood smear in a microscope slide. Images were acquired with Axioskop 2 (Carl Zeiss) with HBO 100 lamps, Axiocam Erc 5 s (Carl Zeiss) and ZEN software (Carl Zeiss) with appropriate laser filter fom TAMRA (filter 4).

3.5. NMR

All NMR experiments were carried out on a Bruker advance III HD 600 MHz. NMR spectra were processed in Bruker TopSpin [14] and analyzed using Sparky [15]. Dimer samples of [C^{13},N^{15}]H2A-H2B at 100 u M in 5 %D_2O/95 %H_2O; 25 mM NaPi + 100 mM NaCl pH6.2 + 0,01 % NaN3 + 1 mM 2-Mercaptoethano + PIC (complete EDTA-free Protease Inhibitor Cocktail (Roche)) were titrated against GMIP1 using 600 MHz Lamour frequency at 308 K. HSQC spectra were measured for free [C^{13},N^{15}]H2A-H2B and after the addition of GMIP1 at 308 K. Titration consisting of 4 points in the range of 1:4.3 M ratio ([C^{13},N^{15}]H2A-H2B:GMIP1) was performed.

3.6. Circular dichroism

Measurement of secondary structure of NBPeps was performed in Jasco *j*-815 spectropolarimeter in a 0,1 cm quartz cuvette in the range of 190 − 250 nm. Samples were diluted in MiliQ water in the concentration of 0.125 mg/mL for GMIP1, LANA, HMGN2 and H4pep at 0.107 mg/mL at 25 ∘C. Data were plotted using BestSel data base (available at: http://bestsel.elte.hu/).

3.7. Computational studies NBPeps

Nucleosome Atomistic models were built using a high-resolution x-ray structure of the nucleosome (NCP) without histone tails, PDB code 3TU4 [16]. Peptides were simulated free in solution or in association with nucleosome at 1:1 and 2:1 stoichiometries. Table M&M provides information on the construction and initial atomic coordinates for the various systems under investigation. Analyses were performed with VMD version 1.9.3 [17].

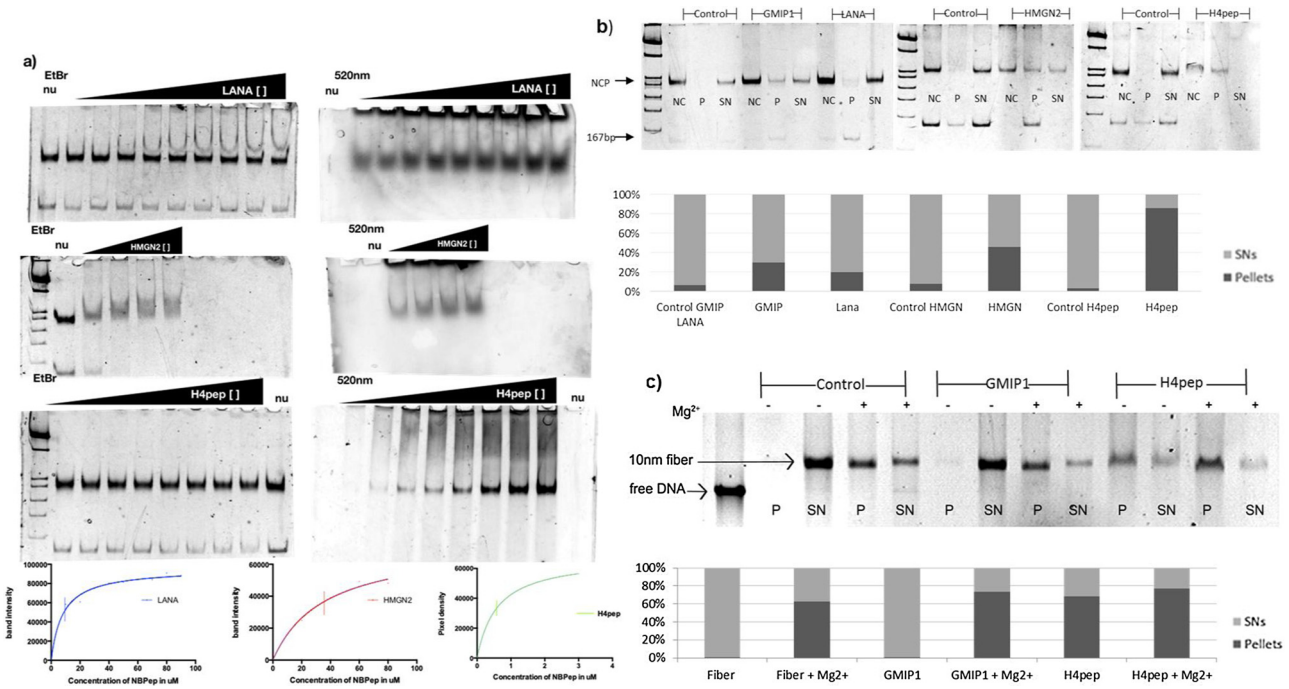

Fig. 1. NBPeps interaction assay a) Nucleosome binding assay with fluorescent NBPeps, nucleosome is incubated with LANA at 0, 10, 20, 30, 40, 50 60, 70 80, 90 u M, with HMGN2pep at 0, 20, 40, 60, 80 u M or with H4pep at 0, 200, 400, 600, 800, 1000, 1200, 1400, 1600 nM. It was then analyzed in acrylamide gel, following by detection of the fluorescent NBPep and subsequently detection of DNA. Kd is represented by a vertical line in the densitometry graphs. b) Nucleosome precipitation assay with NBPeps, centrifuged nucleosome without NBPeps stays in the supernatant (SN); the addition of 50 u M GMIP1, 10 u M LANA, 10 u M HMGN2 or 500 nM H4pep induce precipitation and pellet (P) formation, non-centrifuged (NC) samples were used as control. DNA band densitometry graph of upper gel c) Chromatin compaction assay with Mg2 +, 150 u M H4pep induces 36-mer chromatin precipitation, but not 150 u M GMIP1. DNA band densitometry graph of upper gel. DNA band densitometry graph of upper gel. These assays were performed at least 3 times, and the representative gel was presented.

3.8. Molecular docking

AutoDock Vina was used to resolve peptide binding to the acidic patch region of NCP [18]. To account for a larger ensemble of binding modes 20 independent structures randomly collected from the peptide-free MD equilibration was docked to the NCP. The exhaustiveness value was set to 200 and best solutions were gathered from each docking calculation, resulting in approximately 400 solutions per peptide. Solutions were clustered in 15–17 structural groups based on a maximum neighborhood criterion and the group with best fit to the acidic patch was chosen for further simulation.

3.9. Molecular dynamics simulations

The VMD software was used to solvate and neutralize with counter ions the NCP-peptides systems [17], resulting in simulations cells averaging ~ 110 Å x 145 Å x 145 Å with ~ 210.000 atoms and 150 mM sodium chloride. All systems were simulated in a NPT ensemble at 300 K, 1 atm and with 2 fs time step for 115 ns with periodic boundary conditions (PBC) and enough water to avoid any interactions between the PBC images. Each system was thermalized and subsequently equilibrated for ~ 10 ns MD simulation. All simulations were run by NAMD version 2.10 [19] with CHARMM 36 force field [20] and TIP3 water model [21]. PME method [22] was employed on the electrostatic calculations and non-bonded interactions were cut-off at 11 Å. No bias was needed to keep the peptides bound to NCP throughout the entire simulation.

4. Results

4.1. In silico development and analysis of structure-based nucleosome binding peptide

To design and develop a NBPep that best-fitted on the nucleosome surface, we studied available nucleosome binding proteins structures as templates [5,16,23–25]. We used the software KvFinder to identify putative binding pockets and shallow crevices on the nucleosome surface to use these cavities as potential binding site to plan NBPeps [26]. We selected three crystallographic atomic structures to start our search, those of RCC1, Sir3 and LANA. The best-fitted molecule on the acidic patch was RCC1 (Supplementary Fig. 1a), which contains binding sites for both the acidic patch and the associated nucleosomal DNA [23]. Besides the deep anchor on the acidic patch, through R216 and R223, there is another region distal to the acid patch in which the residue T238 from the RCC1 may interact to T75 from H2A. Therefore, based on the structure of RCC1:Nucleosome complex, we generated the new NBPep, GMIP1 (genetic modified inducible peptide 1), which included the two nucleosome binding sites to either DNA or the acidic patch, linked by three alanine residues (Supplementary Fig. 1 b–d).

4.2. Differential binding of NBPeps to the nucleosome and effect on chromatin conformation

We selected NBPeps based on their abilities to bind to the (i) acidic patch (LANA and H4) or (ii) both DNA and acidic patch (GMIP1 and HMGN2).

We already knew that the NBPeps LANA, H4 tail and HMGN2 could bind to the nucleosome [5,24,25], but we did not have biochemical information about GMIP1. Although GMIP1 was based on the nucleosome binding motif of RCC1, it has a new structure, with two independent binding regions linked by three alananine residues as

discussed earlier. Circular dichroism analysis of the NBPeps showed predominant random coil structure (Supplementary Fig. 2 and Supp. table 1 sequence NBPeps). NMR experiments with free GMIP1 indicated the peptide is in a random-coil state based on absence of medium or long-range NOEs and random coil 13C chemical shifts (Santos GM and van Ingen H., personal communication).

To observe the binding and the impact of NBPeps to the nucleosome we performed nucleosome binding and precipitation assays (Fig. 1 a). First, we reconstituted nucleosomes *in vitro* with histone octamer from chicken and 167.1 (167 base pairs) DNA 601 and incubated it with labelled NBPeps-TAMRA. It demonstrated that H4pep binds to the mononucleosome at a Kd of 0,6 u M, LANA at Kd of 8 u M and HMGN2 at 358 u M respectively. GMIP1 induced nucleosome aggregation even in low concentration, which difficulted to determine the binding affinity constant. HMGN2pep promotes an electrophorectic mobility shift, suggesting that it is binding at more than one site on the nucleosome surface, further investigations will be need to explore this finding.

To confirm the binding assays results, non-labelled GMIP1, LANA, HMGN2 and H4pep were then incubated with mononucleosomes and then centrifuged. We observed that the nucleosome in absence of NBPeps does not precipitate, but all four NBPeps variably induced nucleosome precipitation since part of the complex was found in the pellet (Fig. 1 b). Notable, H4pep induced precipitation at 500 nM. At higher concentration, the NBPeps induce mononucleosome aggregation and did not migrate in the gel (data not shown).

To understand and validate the binding epitope of GMIP1 on the histone H2A:H2B surface, we performed an interaction study with *in vitro* reconstituted and isotope-labeled *xenopus laevis* H2A/H2B dimers by NMR. Binding of unlabeled GMIP1 should result in specific and clear changes in either peak position and/or intensities. Surprisingly, no significant spectral changes were observed even at high excess of GMIP1 (Supplementary Fig. 1 e), suggesting that this new NBPep needs DNA binding to be stable on the nucleosome. Indeed, GMIP1 bound to the naked DNA *in vitro* (Supplementary Fig. 1 f) but at a Kd of 50μM or weaker, which is probably in the range of non-specific binding of a charged peptide to DNA. Furthermore, GMIP1 showed to induce nucleosome aggregation which difficulted the Kd determination. Nucleosome (Supplementary Fig. 1 g). We then applied docking and Molecular Dynamics simulations to study binding of the GMIP1 at the atomic level and the conformational stability of the nucleosome. It showed that H2A/H2B dimer is not sufficient to hold GMIP1 on the nucleosome. Interestingly, the nucleosomal DNA stabilizes GMIP1 on both DNA and H2A/H2B dimer (Supplementary video and Supplementary Fig. 3).

It is already known that the non-acetylated H4 tail is able to induce chromatin condensation. [27].In order to check whether GMIP1, which low affinity nucleosome binding is similar to LANA and HMGN2pep, could also affect the chromatin state such as described for non-acetylated H4 tail, we performed a chromatin compaction assay with Mg^{2+} (Fig. 1 c). For this, we reconstituted long chromatin fibers, 177.36 (36 nucleosomes), *in vitro* and incubated them with H4pep and GMIP1 and then with Mg^{2+}, following to centrifugation. Since the precipitated chromatin fiber recovered from the pellet was not cross-linked, it did not hold the compacted state and migrated in the gel similarly to the relaxed chromatin fiber, as observed in the gel. H4pep induced precipitation even in absence of Mg^{2+}, and precipitation increased when the divalent cation was added. However, GMIP1 did not show any effect alone, even when it was in presence of Mg^{2+}.

Taguchi et al. have established a technique to evaluate the physical properties of nucleosomes, developing a convenient assay of the thermal stability of nucleosomes *in vitro*. It was observed that increasing temperature induces nucleosome denaturation in two steps, firstly at 75 °C the eviction of H2A:H2B dimers occurs followed by the eviction of H3:H4 tetramers at and at 85 °C [11]. Therefore, herein thermal shift assays were performed to further check the hypothesis that NBPeps affect nucleosome stability (Fig. 2). GMIP1 showed a dose dependent effect of the nucleosome stability, affecting first the H2A:H2B dimers, with a pronounced effect at higher concentrations, 150 u M. LANA has a notable effect on the H3:H4 tetramers, starting at 30 u M. HMGN2 induced earlier disruption of the H3:H4 tetramers at 3 u M. Clearly, H4pep induced H2A:H2B dimer stabilization at 100 nM concentration and did not affect H3:H4 tetramer. These findings suggested that NBPeps affect the nucleosome stability in different manners, however only H4pep presented a high specificity effect.

4.3. The interaction mode of NBPeps and nucleosome

In order to understand how the nucleosome structure senses the binding of NBPeps, MD simulations were performed to study the NBPeps based on their abilities to bind to the acidic patch or both DNA and acidic patch. More specifically, we studied peptide motifs from LANA and H4 tail that just bind to the H2A and H2B of the acidic patch and, for the second group, the peptide motif from HMGN2 and the new GMIP1 that bind to H2A and H2B and DNA. A scrambled peptide derived from GMIP1 was used as a negative control. All NBPeps tested here, but not the negative control, were able to bind and maintain the interaction with nucleosome over 115 ns of equilibrium trajectory (Fig. 3a).

It was observed that NBPeps induced specific atomic fluctuations of the nucleosome structure. Based on the differences of RSMF (root square mean fluctuation) of the nucleosomes, in presence and absence of the NBPeps, a map of the fluctuations was generated. There were several common fluctuation changes caused by the different NBPeps, however it is important to highlight the fluctuations of two distinct regions of the nucleosome (circles and arrows Fig. 3b). First, NBPeps that interact with just the acidic patch caused higher atomic movement at the nucleosome entryside-DNA region (arrows Fig. 3b). LANA significantly increase the DNA atomic fluctuations and H4pep slightly increase fluctuations of the H3 N-terminal helix. As expected, GMIP1, but not HMGN2, which also bind to the DNA, moderately reduced the DNA fluctuation. The second region affect by NBPeps binding was one of the known interactions points between the DNA and histones [25] (circles Fig. 3b). This interface, composed by H4 amino acids A76, K77, R78 and 8 nucleotides, showed narrow movement reduction caused by all NBPeps. Also, although rather small, HMGN2 was the peptide with greater impact (increasing) on the histones octamer atomic fluctuations.

Changes in hydration pattern of the nucleosome showed that the NBPeps reduced at least water content by 10 % on the acidic patch. GMIP1 removed fewer water molecules compared to the other NBPep, even when compared to HMGN2 that also has two binding sites, DNA and acidic patch (Fig. 3c).

4.4. NBPeps cellular uptake and viability

Cell penetrating peptides, CPPs, are typically short peptides composed by high content of positively charged amino acids, such as lysine and arginine. Interestingly, NBPeps also contain several positively charged aminoacids [28]. In order to verify whether the four NBPeps could penetrate the cell environment, we performed flow cytometry assays in Hela cells. The four NBPeps penetrated the cell at 37 °C and GMIP1 had the highest uptake. H4pep in higher concentration (10 u M) was also taken up at 4 °C at a similarly rate to 37 °C (Fig. 4a).

To better understand and characterize whether GMIP1 that presented low affinity nucleosome binding could be uptaken and bind to the chromatin, we treated Hela cells with labeled GMIP1 and analyzed them with confocal microscopy. Images with orthogonal views demonstrated that peptide GMIP1 penetrates the cells even in the smallest concentration (0.1μM). Confocal microscopy merged images of labeled GMIP1 and DNA stained with DAPI indicate the presence of GMIP1 associated with chromatin (Fig. 4b). Internalization of GMIP1 in Hela cells occurred only at 37 °C, suggesting an endocytosis transport

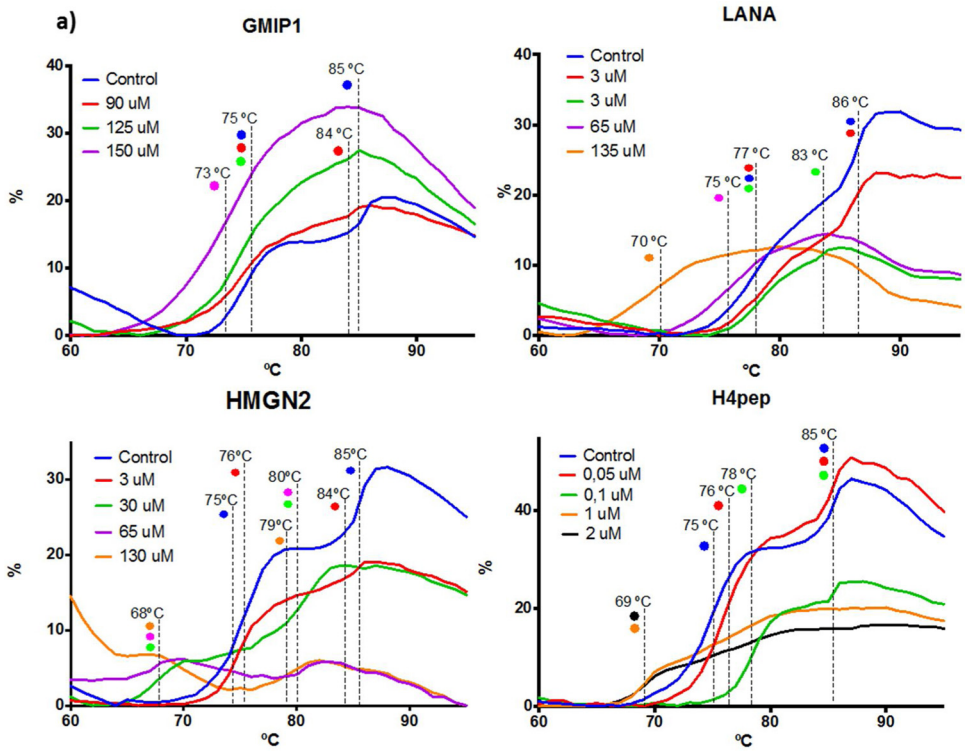

Fig. 2. Thermal Shift assay a) Thermal denaturation profiles of mononucleosomes in the presence of NBPeps. Mononucleosome denaturation happens in two steps, the first peak is the eviction of the dimers H2A/H2B and the second step if the eviction of the tetramers H3/H4 the formation of a peak at 68 – 70 °C appears when the mononucleosome is already disassembled. All thermal denaturation profiles are representative of three separate experiments.

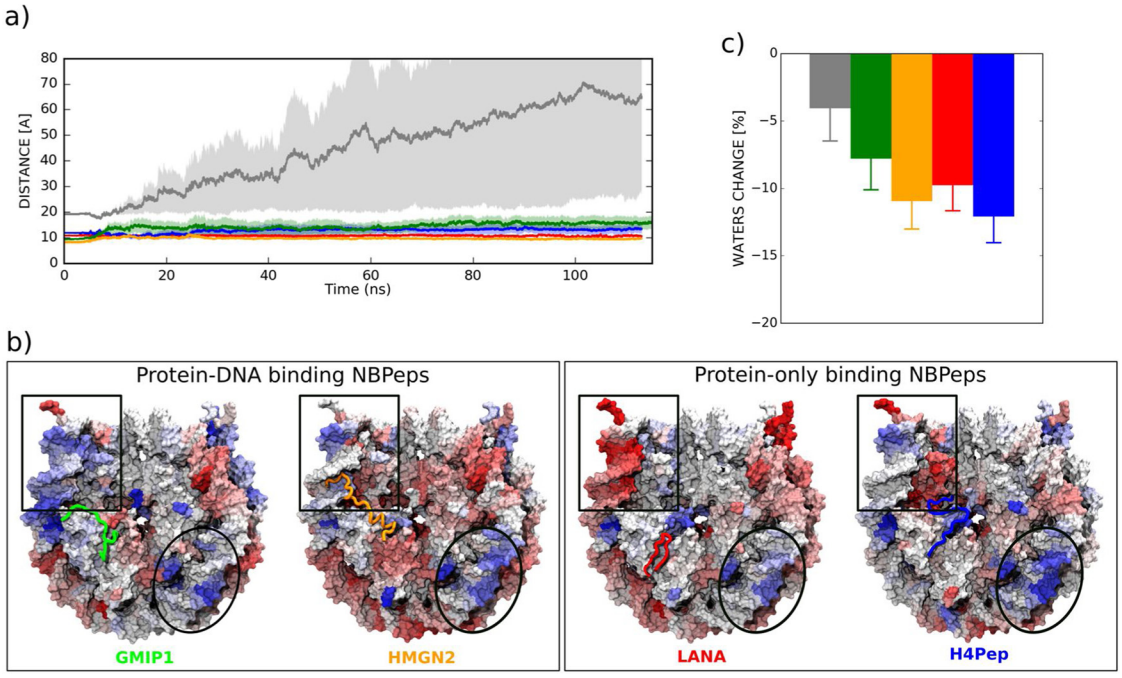

Fig. 3. NBPeps interactions with the nucleosome a) Time-dependent centroid distances profiles between the acidic patch region and NBPeps (Negative control – gray; GMIP1- green; HMGN2 – orange; LANA – red; H4pep - blue). Shaded regions indicate standard error between all simulations. b) NBPeps-induced proportional changes on the nucleosome (NCP) root-mean-square fluctuations (RMSF). The ratio was calculated after averaging all peptides association with the nucleosome stoichiometries. Color scale values distinguish between higher (red) and lower (blue) fluctuations compared to the RMSF of NBPep free nucleosome, with a 25 % cut-off. Squares and circles indicate strongest fluctuation changes regions **c**) Average of proportional change in the number of water molecules occupying the acidic patch for each NBPep. The change was calculated using the nucleosome free simulation as base value and within a cut-off distance of 20 Å. Averages and associated standard deviation were computed from 100 ns simulation. Colors code as a).

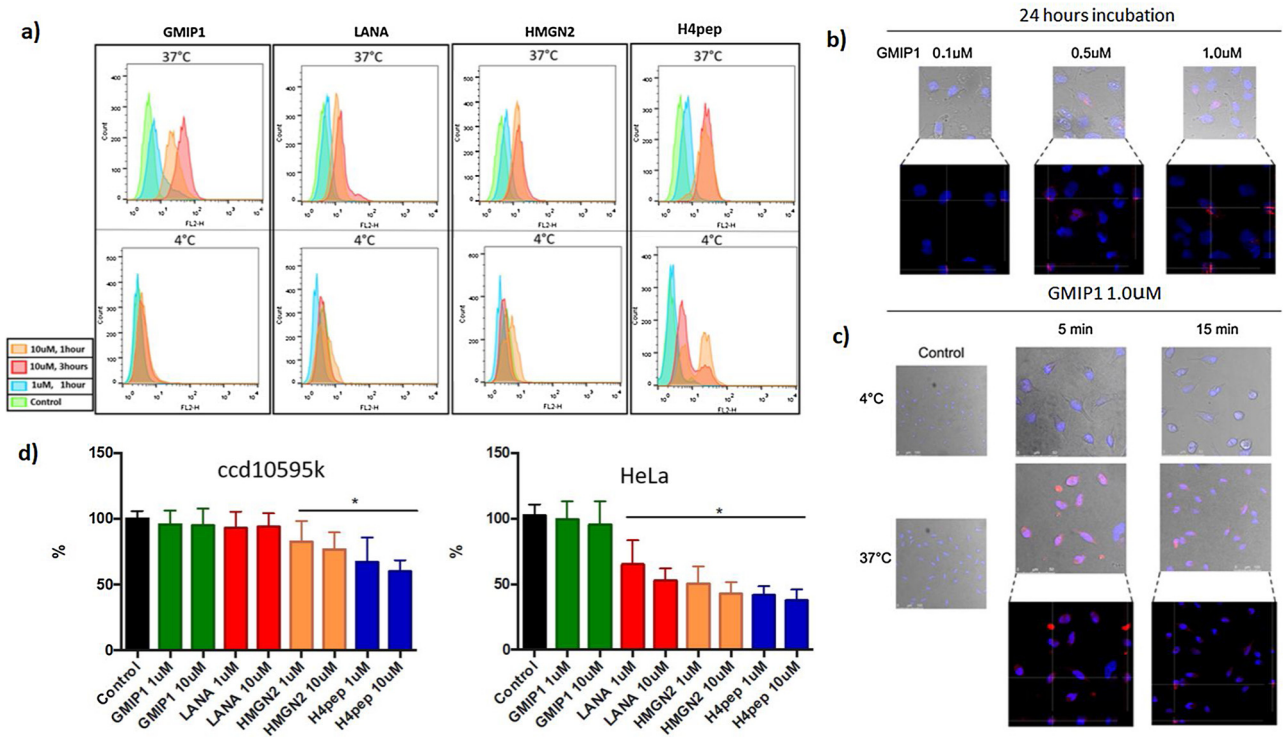

Fig. 4. NBPeps cell penetration a) Flow cytometry profile of Hela cells uptake of fluorescent NBPeps (TAMRA), in histogram view with 1 or 3 h exposure and at 37 or 4 °C. Histogram is representative of three separate experiments.
b) GMIP1 bound to chromatin: confluent Hela cells were treated with increased concentrations (0.1; 0.5; 1μM) of peptide GMIP1-TAMRA or vehicle (10 mM Tris – HCl) for 24 h. The images were acquired using a laser scanning confocal microscope Leica TCS SP5. C) GMIP1 internalization: Ortogonal analysis of GMIP1 overlapping with stained (DAPI) DNA. Cell penetration only occurs at 37 °C. The images were acquired using a laser scanning confocal microscope Leica TCS SP5. To visualize peptide localization, Z-planes of 0.20 μm thickness were acquired. The software LAS AF (Leica Microsystems CMS GmbH) was used for analyze images. All images are representative of three separate experiments. d) Relative cell viability compared to control over 24 h exposure to NBPeps in HeLa and CCD 10,595 K. HeLa cells showed a greater decreased in cell viability than CCD 10595k for every NBPep tested with the exception of GMIP1. Data is shown as mean ± SD. * represent significant statistical difference (one-way ANOVA test) between the control and treated groups with = $p < 0.05$ and $n = 2$.

(Fig. 4c).

4.5. Cell viability assay with NBPeps

In order to verify the potentiality of NBPeps for modulating cell physiology, we performed MTT assay using with different cell linages. In general, NBPeps, but not GMIP1, significantly affected the viability of Hela cells, which support the evidences obtained *in vitro* that GMIP1 is acting non-specifically. Furthermore, NBPeps impacted the primary cell lineage ccd10595k much less, except H4pep that still showed high effect on the cell viability (Fig. 4d).

5. Fish embryo toxicity (FET) with NBPeps

To analyze *in vivo* the action of the NBPeps, we performed we performed Fish Embryo Toxicity (FET, OECD protocol n.236, 2013) test. After the exposure to NBPeps, at 3 different stages of development, at 4, 28 and 52 h post-fertilization (hpf) for 1 and 24 h, all NBPeps presented low or no toxicity (Supplementary table 2).

We were able to identify the labeled NBPeps in the nuclei of adult zebrafish erythrocyte (Fig. 5a). Moreover, NBPeps penetrated different tissues of fish larvae, after 3 hs incubation (Fig. 5b).

The respective outcome of the embryo's exposure to the NBPeps was highly dependent on the stage of development (Fig. 5c). The hatching rate of the zebra fish was largely affected by the presence of the NBPeps, with GMIP1 showing the strongest effect (Supplementary table 2).

GMIP1 presented a discrete pigmentation defect, in 26 % of embryos when at 28hpf and did not induce mortality at any concentration tested.

LANA, at the highest concentration (100 u M), caused delay in the development of 100 % of the embryos when they were exposed at 4hpf. Also, LANA induced an increased hatching rate (Fig. 5c and Supp. table 2).

HMGN2 clearly affected pigment formation of 16 % of the embryos at 100 u M when at 56hpf.

Remarkably, H4pep were the only NBPeps tested that induced 100 % mortality at 4hpf, and the exposure for 1 h induce 20 % of mortality.

6. Discussion

Proteins that bind the nucleosome, the repetitive unit of chromatin, and the histone H4 tail are critical for establishing chromatin architecture and phenotypic outcomes [29]. A myriad of histone modifications, which strongly induce changes in chromatin structure, have been associated with malignancies and other diseases, highlighting the crucial role of chromatin architectural changes in disease mechanisms [30]. Thus, it is plausible that any nucleosome binding molecule might be able to interfere with the chromatin dynamics and modulate the access of proteins to the DNA.

At first glance, small molecules would be the best option for engaging the nucleosome surface, mainly the acidic patch, to control chromatin dynamics. An effort to identify specific inhibitors of Kaposi's sarcoma–associated herpesvirus (KSHV) focused on small molecules that could displace the LANA peptide from the acidic patch [31]. Investigators tested more than 350.000 small molecules, but could not find any compound able to displace LANA from the nucleosome surface, suggesting that more complex molecules, such as peptides, might be

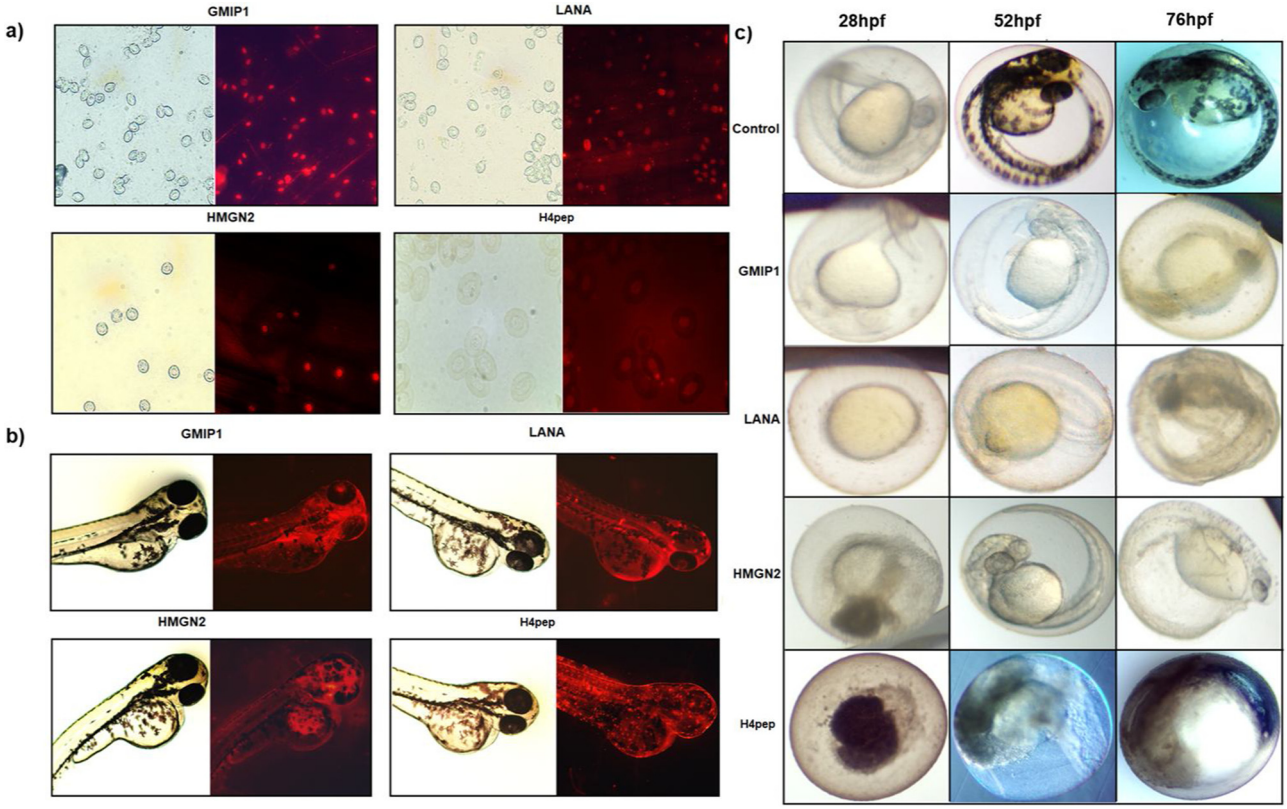

Fig. 5. NBPeps action *in vivo* a) Injection of fluorescent NBPeps accumulate in the nucleus erythrocytes of adult zebrafish, b) fluorescent NBPeps incubated for 3 h distributes heterogeneously over zebrafish larvae. At right panel, visualization using 520 nm laser. c) Fish Embryo Toxicity (FET) with NBPeps. Zebrafish embryos at 4, 28 and 52 h post fertilization (hpf) were incubated with NBPeps or vehicle for 24 h. Images are representative of three separate experiments.

required to bind in shallow crevices that mediate protein-protein interactions. Recently, binuclear ruthenium compounds was shown to be able to target the nucleosome surface and induce chromatin condensation [32].

Herein, we rationalized that NBPeps would be important candidates for occupying the nucleosome surface and to direct control the chromatin status and phenotypic outcomes. For that, NBPeps derived from binding motifs of structure-characterized nucleosome binding proteins, LANA, H4 tail, HMGN2 and the newly generated GMIP1, were tested to verify their ability in impacting the nucleosome stability, chromatin status, cell viability and fish embryo development. The four NBPeps bound to the nucleosome and induce precipitation at uM order, except H4pep that act at 500 nM.

We first searched for a novel NBPep that could bind to and present specificity for the nucleosome, with high dependence on nucleosomal DNA for the nucleosome binding. This characteristic could potentially open an avenue for the design of NBPeps with high specificity for target genes. However, the biochemical data shows that GMIP1 has low nucleosome binding affinity. It is important to emphasize that all experiments performed were done with the Widom 601 DNA sequence, which is an artificial sequence with high specificity to the octamer.

In general, the NBPeps displaced at least 10 % of the water associated with the acidic patch. Interestingly, thermal shift assays suggest that GMIP1 and HMGN2pep, which also bind to the nucleosomal DNA, primarily disrupt H2A:H2B dimer. This is partially in agreement with the molecular dynamic experiments, in which the HMGN2pep increased histones atomic fluctuations and reduced DNA fluctuation changes at the nucleosome entry-side DNA region. LANA firstly disturb H3:H4 tetramer and H4pep induced H2A:H2B dimer stabilization but did not affect H3:H4. Together with the notion that DNA is needed for GMIP1 binding led us to consider the hypothesis that NBPep with a DNA nucleosomal binding site might be by more effective for modifying the common target on the nucleosome surface. Chromatin compaction was affected by the H4pep but not by GMIP1, supporting the idea that GMIP1 presents low affinity binding to the nucleosome. Cell-based assays demonstrated that all four NBPeps were able to penetrate the cell, with GMIP1 having the best cell uptake. The protein-derived NBPeps, but not the rationally designed GMIP1, significantly affected the viability of tumoral cells. However, NBPeps had weaker effects on the cellular viability of non-tumoral cell lineage, except for H4pep that still showed strong negative effects on cell viability.

Experiments performed in zebrafish showed that NBPeps have a differential interference in the embryo mortality, development, pigmentation and hatching. Labeled NBPeps penetrated different tissues of fish larvae and localized in the nuclei. These results are in agreement to the cell-based assays showing the NBPeps penetrate the cell. It is worthy of attention that GMIP1 did not induce fish embryos mortality, contrarily to H4pep. These data corroborate the results from cell-based assays MTT using non-tumoral ccd 10595k cells. Interestingly, all NBPeps induced earlier hatching, but GMIP1 and LANA induced development embryo delay.

Taken together the *in silico*, biochemical an *in vivo* data, however, it is too early to provide a straight correlation between NBPeps binding sites and the phenotypic outcome. Considering that three out of the four designed peptides are non-specific nucleosomal interactors, a question that is still to be explored is whether the NBPeps may engage different signaling events, besides the nucleosome binding, for example affecting function of HDAC.

Indeed, acetylated H4 N-terminal tail was explored as a molecular tool to establish and maintain the active state of p53 target genes *via* interaction with histone deacetylase 1 (HDAC1). It was suggested that it could be used as a novel strategy for anticancer therapy [33]. Herein, we further advance the idea that H4pep could affect tumoral cells, but through the direct binding to the nucleosome surface, since H4pep was

the unique high specific NBPep, causing dramatic effect *in vivo*. Its effect emphasized the physiological role of H4 tail on chromatin condensation and transcriptional outcome.

In conclusion, we observed that NBPeps with distinct nucleosome binding sites perturb the nucleosome structure in multiple ways. Despite sharing an apparently similar target, NBPeps showed different roles in cell physiology, which is probably due to the non-specificity in targeting the nucleosome surface. However, new biophysical experiments in cell-based context should be performed to be able to straight correlate the *in silico* predictions with the *in vivo* findings.

Nevertheless, considering that DNA intercalaters or damaging agents still have great importance in clinical oncology, the fact that NBPeps do not present specific targeting would not preclude their use as therapeutic agents. Indeed, we believe that NBPeps open novel opportunities to design hybrid molecules with higher specificity to regulate a plethora of cellular disorders.

Declaration of Competing Interest

The authors declare that they have no known competing financial interests or personal relationships that could have appeared to influence the work reported in this paper.

Acknowlegement

The authors are grateful to Carlos Pantoja and Tony Warne for critical reading of the manuscript and anonymous reviewers for the important comments and suggestions on the manuscript. This work has been supported by CNPq for KT,VF and IT fellowships, Fap-DF grant number 04/2017 for GS, iNEXT grant number 6756, funded by the Horizon 2020 programme of the European Union, for HI.

Appendix A. Supplementary data

Supplementary material related to this article can be found, in the online version, at doi:https://doi.org/10.1016/j.biopha.2019.109678.

References

[1] M.R. Hubner, M.A. Eckersley-Maslin, D.L. Spector, Chromatin organization and transcriptional regulation, Curr. Opin. Genet. Dev. 23 (2) (2013) 89–95.
[2] A.A. Kalashnikova, M.E. Porter-Goff, U.M. Muthurajan, K. Luger, J.C. Hansen, The role of the nucleosome acidic patch in modulating higher order chromatin structure, J. R. Soc. Interface 10 (82) (2013) 20121022.
[3] I.T.G. Silva, V. Fernandes, C. Souza, W. Treptow, G.M. Santos, Biophysical studies of cholesterol effects on chromatin, J. Lipid Res. (2017).
[4] J.T. Finch, A. Klug, Solenoidal model for superstructure in chromatin, Proc. Natl. Acad. Sci. U.S.A. 73 (6) (1976) 1897–1901.
[5] A.J. Barbera, J.V. Chodaparambil, B. Kelley-Clarke, V. Joukov, J.C. Walter, K. Luger, et al., The nucleosomal surface as a docking station for Kaposi's sarcoma herpesvirus LANA, Science 311 (5762) (2006) 856–861.
[6] W.F. Cabral, A.H. Machado, G.M. Santos, Exogenous nucleosome-binding molecules: a potential new class of therapeutic drugs, Drug Discov. Today 21 (5) (2016) 707–711.
[7] J.B. Murphy, M.W. Kies, Note on spectrophotometric determination of proteins in dilute solutions, Biochim. Biophys. Acta 45 (1960) 382–384.
[8] P.N. Dyer, R.S. Edayathumangalam, C.L. White, Y. Bao, S. Chakravarthy, U.M. Muthurajan, et al., Reconstitution of Nucleosome Core Particles From Recombinant Histones and DNA. Methods Enzymol. 375, Academic Press, 2003, pp. 23–44.
[9] V.A. Huynh, P.J. Robinson, D. Rhodes, A method for the in vitro reconstitution of a defined "30 nm" chromatin fibre containing stoichiometric amounts of the linker histone, J. Mol. Biol. 345 (5) (2005) 957–968.
[10] B. Dorigo, T. Schalch, K. Bystricky, T.J. Richmond, Chromatin Fiber folding: requirement for the histone H4 N-terminal tail, J. Mol. Biol. 327 (1) (2003) 85–96.
[11] H. Taguchi, N. Horikoshi, Y. Arimura, H. Kurumizaka, A method for evaluating nucleosome stability with a protein-binding fluorescent dye, Methods. 70 (2-3) (2014) 119–126.
[12] OECD. Test No. 236: Fish Embryo Acute Toxicity (FET) Test, OECD Guidelines for the Testing of Chemicals, Section 2, OECD Publishing, Paris, 2013.
[13] M.G. Morash, S.E. Douglas, A. Robotham, C.M. Ridley, J.W. Gallant, K.H. Soanes, The zebrafish embryo as a tool for screening and characterizing pleurocidin host-defense peptides as anti-cancer agents, Dis. Models Mech. 4 (5) (2011) 622–633.
[14] F. Delaglio, S. Grzesiek, G.W. Vuister, G. Zhu, J. Pfeifer, A. Bax, NMRPipe: A multidimensional spectral processing system based on UNIX pipes, J. Biomol. NMR 6 (3) (1995) 277–293.
[15] W. Lee, M. Tonelli, J.L. Markley, NMRFAM-SPARKY: enhanced software for biomolecular NMR spectroscopy, Bioinformatics 31 (8) (2015) 1325–1327.
[16] K.J. Armache, J.D. Garlick, D. Canzio, G.J. Narlikar, R.E. Kingston, Structural basis of silencing: Sir3 BAH domain in complex with a nucleosome at 3.0 A resolution, Science 334 (6058) (2011) 977–982.
[17] W. Humphrey, A. Dalke, K. Schulten, VMD: visual molecular dynamics, J. Mol. Graph. Model. 14 (1) (1996) 27–28 33-8.
[18] O. Trott, A.J. Olson, AutoDock Vina: improving the speed and accuracy of docking with a new scoring function, efficient optimization, and multithreading, J. Comput. Chem. 31 (2) (2010) 455–461.
[19] J.C. Phillips, R. Braun, W. Wang, J. Gumbart, E. Tajkhorshid, E. Villa, et al., Scalable molecular dynamics with NAMD, J. Comput. Chem. 26 (16) (2005) 1781–1802.
[20] J. Huang, A.D. MacKerell Jr, CHARMM36 all-atom additive protein force field: validation based on comparison to NMR data, J. Comput. Chem. 34 (25) (2013) 2135–2145.
[21] P. Mark, L. Nilsson, Structure and dynamics of the TIP3P, SPC, and SPC/E water models at 298 K. J, Phys. Chem. A. 105 (43) (2001) 9954–9960.
[22] T. Darden, D. York, L. Pedersen, Particle mesh Ewald: An N·log(N) method for Ewald sums in large systems, J. Chem. Phys. 98 (12) (1993) 10089–10092.
[23] R.D. Makde, J.R. England, H.P. Yennawar, S. Tan, Structure of RCC1 chromatin factor bound to the nucleosome core particle, Nature. 467 (7315) (2010) 562–566.
[24] H. Kato, H. van Ingen, B.R. Zhou, H. Feng, M. Bustin, L.E. Kay, et al., Architecture of the high mobility group nucleosomal protein 2-nucleosome complex as revealed by methyl-based NMR, Proc Natl Acad Sci U S A. 108 (30) (2011) 12283–12288.
[25] K. Luger, A.W. Mader, R.K. Richmond, D.F. Sargent, T.J. Richmond, Crystal structure of the nucleosome core particle at 2.8 A resolution, Nature 389 (6648) (1997) 251–260.
[26] S.H. Oliveira, F.A. Ferraz, R.V. Honorato, J. Xavier-Neto, T.J. Sobreira, P.S. de Oliveira, KVFinder: steered identification of protein cavities as a PyMOL plugin, BMC Bioinformatics 15 (1) (2014) 197.
[27] P.J. Robinson, W. An, A. Routh, F. Martino, L. Chapman, R.G. Roeder, et al., 30 nm chromatin fibre decompaction requires both H4-K16 acetylation and linker histone eviction, J. Mol. Biol. 381 (4) (2008) 816–825.
[28] H. Derakhshankhah, S. Jafari, Cell penetrating peptides: a concise review with emphasis on biomedical applications, Biomed. Pharmacother. 108 (2018) 1090–1096.
[29] C.L. Woodcock, Chromatin architecture, Curr. Opin. Struct. Biol. 16 (2) (2006) 213–220.
[30] A.C. Mirabella, B.M. Foster, T. Bartke, Chromatin deregulation in disease, Chromosoma 125 (1) (2016) 75–93.
[31] C. Beauchemin, N.J. Moerke, P. Faloon, K.M. Kaye, Assay development and high-throughput screening for inhibitors of Kaposi's sarcoma-associated herpesvirus N-Terminal latency-associated nuclear antigen binding to nucleosomes, J. Biomol. Screen. 19 (6) (2014) 947–958.
[32] G.E. Davey, Z. Adhireksan, Z. Ma, T. Riedel, D. Sharma, S. Padavattan, et al., Nucleosome acidic patch-targeting binuclear ruthenium compounds induce aberrant chromatin condensation, Nat. Commun. 8 (1) (2017) 1575.
[33] K. Heo, J.S. Kim, K. Kim, H. Kim, J. Choi, K. Yang, et al., Cell-penetrating H4 tail peptides potentiate p53-mediated transactivation via inhibition of G9a and HDAC1, Oncogene. 32 (20) (2013) 2510–2520.